Cold-sprayed Coatings based on High Strength Aluminium alloys Reinforced by Quasicrystalline Particles: Microstructure and Key Properties

A.V. Byakova, M.M. Kiz, A. I. Sirko, M. S. Yakovleva and Yu. V. Milman*

Institute for Problems of Materials Science, Ukrainian National Academy of Sciences, 3 Krzhyzhanovsky St., 03142, Kiev, Ukraine

(Received March 20, 2010 ; Final form June 6, 2010)

ABSTRACT

This study presents significant advantages of cold-spraying in performance of coatings based on Al matrix reinforced by metastable nano- and submicrosized quasicrystalline particles as compared to those processed by thermal spraying and, in particular, by high velocity oxy-fuel (HVOF) spraying technique. Two kinds of feedstock powders with nominal compositions $Al_{94}Fe_3Cr_3$ and $Al_{94}Fe_{2.5}Cr_{2.5}Ti_1$ were employed in spraying the coatings on cold rolled steel substrate. Microstructure and key mechanical characteristics of feedstock powders and coatings performed by cold-spraying and HVOF process were studied and discussed. The main benefit of cold-spraying as opposed to HVOF spraying was that the composite quasicrystalline structure of initial feedstock powders is retained in the interior of flattened particles heavily deformed under impact in solid state. Strain hardening of coating and substrate is resulted from impact during cold-spraying. The results showed that unlike to HVOF sprayed coatings important advantage of cold-sprayed quasicrystalline coatings is referred to combination of increased hardness with ductility indicated by plasticity characteristic just about critical value $\delta_H \approx 0.9$, which is quite enough for preventing brittle failure of material during particle impact onto substrate or previously deposited particles.

E-mail: maximkiz@gmail.com (M.M. Kiz)

Keywords: Cold spraying; Thermal spraying; Quasicrystalline Al alloys; Microstructure; Mechanical properties, Bond strength

1. INTRODUCTION

Quasicrystals as a new class of solids with unusual quasiperiodic atomic structure /1/ exhibit unique physical, chemical, and mechanical properties, making them of growing attention for researchers employed in scientific and engineering applications. In particular, Al-based quasicrystalline materials demonstrate relatively low density roughly about 4.5 g/cm^3, high hardness ranging from 4 to 10 GPa, high Young's modulus ranging from 70 to 100 GPa, low thermal conductivity, low friction, and oxidation resistance /2-7/. Among other valuable properties high elevated-temperature strength indicative of nanoquasicrystalline alloys in Al-Fe based systems /3, 8 – 14/ is important for different applications and, especially, for application in aircraft industry.

Unfortunately, single-phase quasicrystalline solids are of brittle nature /3/. State-of the-art quasicryactalline alloys consist of α-Al matrix reinforced by nano-sized quasicrystalline particles show remarkable advantages in material mechanical performance, allowing for combination of high strength and sufficient ductility /10, 15 -17/.

Generally, rapid solidification technique with high cooling rate about 10^5 K/s is required to create

quasicrystalline phases /3, 11, 18, 19/. Metastable state is indicative of quasicrystalline phases although stable quasicrystals are also found /3/. A number of processing routes including rapid quenching /20, 21/, centrifugal atomisation /22, 23/, crystallisation of amorphous alloy /24/, spray forming /25/, etc. are presently available for synthesis of Al-based quasicrystalline alloys while powder atomisation technique either with argon-gas /11, 26/ or inhibited water /10, 17/ are thought to be mostly effective for mass production. When quasicrystalline alloy is performed as semi-product in form of powder/flakes their following consolidation is required to manufacture the bulk material.

Plasma spraying and high velocity oxy-fuel (HVOF) flame spraying technique are commonly applied for performance of Al-based quasicrystalline material in form of coating /3, 16, 26-33/. These thermal spraying processes exhibit high deposition efficiency although they have several technical limitations as applied to performance of quasicrystalline coatings and especially those based on Al matrix reinforced by metastable quasicrystalline phases. In thermal spray processes, phase transformation can occurs since the sprayed material is at least partially molten because of extremely high temperatures which are typically achieved up to 2000... 5000° C as in HVOF process or 3000 ... 20000° C as in plasma spraying /34/. Oxidation can occur during the flight through the nozzle and the free gas jet, and also it can take place during solidification on the substrate /10/. Moreover, thermal spraying can result in Al evaporation loss, causing undesirable alteration of alloy elementary composition.

Powder metallurgical (PM) route using extrusion technique is alternative process for consolidation of powdered quisicrystalline alloy by plastic deformation. There are two different PM processes performed either in hermetic chamber with argon gas /11/ or degassing capsule /10, 16/. Although PM route offers indisputable advantages in term of retaining the elementary balance in quasicrystalline alloy as well as avoiding the oxidation and phase transformation it is rather complicated and expensive for industrial application.

Cold spraying recently developed in the family of thermal spray processes /35, 36/ offers wide scope in performance management and volume production of quasicrystalline material and coating. In this process feedstock powder particles are accelerated to supersonic velocities by a highly pressurised gas jet generated through a convergent-divergent Laval-type nozzle at the temperature well below the melting point of the sprayed material. Thus, cold spraying is a solid-state process which results in coating formation by intensive plastic deformation similar to that indicative of PM route, as was shown in previous paper /16/. However, cold spraying process is yet imperfectly characterised in respect to performance of quasicrystalline coatings although its efficiency in deposition of many other metallic coatings including nanostructured ones has been justified /37-43, 45/.

This paper demonstrate the capabilities and advantages of cold spraying in performance of Al-based quiasicrystalline coatings by comparing their structure and key properties with those of thermally sprayed coatings.

2. EXPERIMENTAL

2.1 Powder and Coating Preparation

Quasicrystalline powders of two aluminium alloys with nominal compositions of $Al_{94}Fe_3Cr_3$ and $Al_{94}Fe_{2.5}Cr_{2.5}Ti_1$ were chosen as sprayed materials /10/. Powders of Al-alloys with oxygen content about 0.3% were fabricated by water –atomisation technique using inhibited high-pressure water with Ph 3.5 /44/. As compared to conventional gas-atomisation process, water-atomisation process provides advantages in higher cooling rates up to 10^6 K/s although the oxygen content (0.2%) is almost the same. After atomisation the powders were sieved to less than 40 μm in size using the corresponding sieves.

Coatings were performed both by cold spray technique and HVOF spraying. A commercial cold spray system (DYMET 403) was used in spray experiments. In this system, preheated propellant gas is driving through Laval nozzle to get a supersonic gas/particle jet. High-pressure compressed air was used both as the propellant gas unlike the other studies, which provide application of inert gases such as argon or helium in cold spraying the Al-alloy powders /39, 41,

46/. Atomised Al particles are often covered by oxide layer of nanosized thickness that originated from water medium as well as from oxygen contamination of inert gas. The dense oxide layer interfere further oxidation of Al-powder, making the demands to oxidation prevention of small importance. Feedstock Al-powder was injected into the supersonic jet from radial direction behind the throat of the nozzle by Venturi effect. Standoff distance was set at 10 mm in front of the spray gun to built-up the coating on the substrate. Principle and technical set-up for cold spraying are described elsewhere /35/.

HVOF spraying was performed with well-established combination of feedstock powder and gas conditions using "Peryn-C" apparatus. In this system acetylene-oxygen mixture was used as an explosive fuel gas. Spray conditions accepted in the experiments are summarised in **Table 1**.

Table 1
Spray parameters of cold spraying (CS) and high velocity oxy-fuel (HVOF) process

Process	Feedstock Powder	Process gas	Velocity, m/s	Standoff Distance, mm	Inlet Temperature, °C	Pressure, MPa
CS	0-40 μm $Al_{94}Fe_3Cr_3$ $Al_{94}Fe_{2.5}Cr_{2.5}Ti_1$	Compressed Air	700	10	<200	0,8
HVOF	0-40 μm $Al_{94}Fe_3Cr_3$ $Al_{94}Fe_{2.5}Cr_{2.5}Ti_1$	O_2+C_2H_2+air	900 -1000	110	2500	-

Cold rolled plates of low carbon steel (carbon content 0.2 %) with a thickness about 3.0 mm were used as substrates and they were sand-blasted prior to spraying. Substrate overall dimensions and coating thickness were chosen with regard to further investigations.

2.2 Powder and Coating Characterisation

Composition of feedstock powder and coating were examined by X-ray diffraction (XRD) analysis using Cu K_α radiation. Scanning electron (SEM) microscope Jeol Superprobe-733 (JEOL, Japan) equipped with X-ray detectors (EDX and EPMA) was used to recognise feedstock powder morphology (particle size and shape) and microstructure as well as to get basic information about coating thickness, porosity, microstructure, and also particle/substrate and particle/particle bonding. Transmission electron microscopy (TEM) images and selected area electron diffraction (SAED) patterns being performed using JEM 2100 F (JEOL, Japan) microscope were also analysed to study structural features of sprayed coatings. Coating porosity was determined by image analysis of the cross-section samples.

Prior to SEM observation feedstock powder was glued by conductive compound and prepared by standard metallographic technique with polishing by diamond slurry. The same polishing procedures were used to prepare surface and cross-sections of coatings jigged in cramps.

2.3 Mechanical Properties

Hardness measurements and bond strength tests were used to characterize coating mechanical properties. Coating plasticity was also determined in addition to microhardness as a measure of material strength.

Hardness measurements were performed on polished cross-sections of coatings in the as-sprayed state using conventional microhardness machine equipped by standardised Vickers pyramid. In addition, polished steel substrate and polished sample of glued feedstock powder were also subjected to hardness measurements. Microhardness values of tested materials were determined under loads higher than critical value $F \geq F_c$ to avoid uncertainty in comparison of measurement results caused by the size effect, as was proposed in /47/. Since critical indentation load F_c is variable value that

depends on solid composition and structure /47, 48/ it was found in preliminary indentation experiments with all materials of interest. According to the test method procedure microhardness numbers were determined in wide range of indentation loads and then they were truncated to define area corresponded to results measured under $F > F_c$ where dependence of HV on F is negligible. Final microhardness numbers determined under the each of indentation loads were averaged over the data obtained by the measuring not less than 10 indentations. Overall, indentation load used in microhardness measurements of powder particles was as high as 0.2 whereas that employed in experimentation with coatings/substrate was about 1.0 N.

Plasticity characteristic δ_H was derived by calculations through microhardness measurement results /49/. According to physical definition δ_H parameter characterises material capability to change the form and defines a share of plastic deformation in total elastic/plastic deformation under indentation. Plasticity characteristic δ_H is dimensionless parameter that can vary in the range from 0 (for "pure" elastic contact) to 1 (for "pure" plastic contact).

Following equation was used for calculation of plasticity characteristic δ_H through Vickers hardness /49/

$$\delta_H = 1 - 14.3\left(1 - \nu - 2\nu^2\right)\frac{HV}{E} \qquad (1)$$

where ν and E are Poison ratio and Young's modulus of tested material, respectively.

Microtester capable for load-displacement measurements and equipped by Berkovich pyramid was used to determine Young's modulus, E, according to the test method procedure originally proposed by Oliver and Pharr /50/. In addition, plasticity characteristic δ_A, which is physically close to that denoted by δ_H /49/ was derived from loading and unloading data according to demands of International standard ISO 14577-1:2002 (E). Maximum indentation load used in load-displacement experiments was as high as 2 N. Principles and test method procedure for determining the plasticity characteristic δ_A, are described in /51-53/. It is noticeable that compared to δ_H parameter determination of plasticity characteristic δ_A offers doubtless advantages because its value is directly derived from experimental data and no evidences concerning the values of Young's modulus and Poison ratio are not required.

According to demands of European standard EN582 bond strength measurements were performed in a tensile mode from the pull-off test. As-sprayed bond strength samples were glued to counter bodies using the adhesive (Loctite, Ireland) with nominal strength up to 70 MPa. Technical set-up for pull-off test is described elsewhere /54/.

3. RESULTS AND DISCUSSION

3.1 Microstructure of Feedstock Powder and Sprayed Coatings

Morphology of as-atomised powder is shown in **Figure 1a**. It could be seen that powder particles have irregular shape typically formed by water-atomisation technique /44/. Compared to spherical shape indicative of gas-atomised powder, irregular shape of water-atomised powder particles offers essential advantages, ensuring higher particle velocity as it was shown for cryomilled powder of Al-alloy /38/ and easier compaction under further consolidation in dense coating.

SEM images for microstructure of as-atomised powder demonstrate a huge numbers of white particles presented in the interior of the powder particles, as shown in **Figure 1b**. The results of XRD analysis indicate quasicrystalline nature of powdered alloy, see **Figure 2a**. In the XRD diffraction pattern of powdered alloys strong diffraction peaks attributed to icosahedral phase (further denoted as i-phase) are revealed besides diffraction peaks of α-Al. In $Al_{94}Fe_3Cr_3$ alloy increased content of Fe and Cr is detected in quasicrystalline particles by EDX analysis whereas the presence of titanium is additionally detected in quasicrystalline particles of $Al_{94}Fe_{2.5}Cr_{2.5}Ti_1$ alloy. Elementary composition of quasicrystals in $Al_{92.5}Fe_{2.5}Cr_{2.5}Ti_{2.5}$ alloy was thought to be compositionally corresponded to $Al_{75}Fe_{13}Cr_{11}Ti_1$ compound /55/.

Size of quasicrystalline particles typically varies from 50 to 200 nm although quasicrystalline particles with the size increased up to 1.5 μm are also revealed in

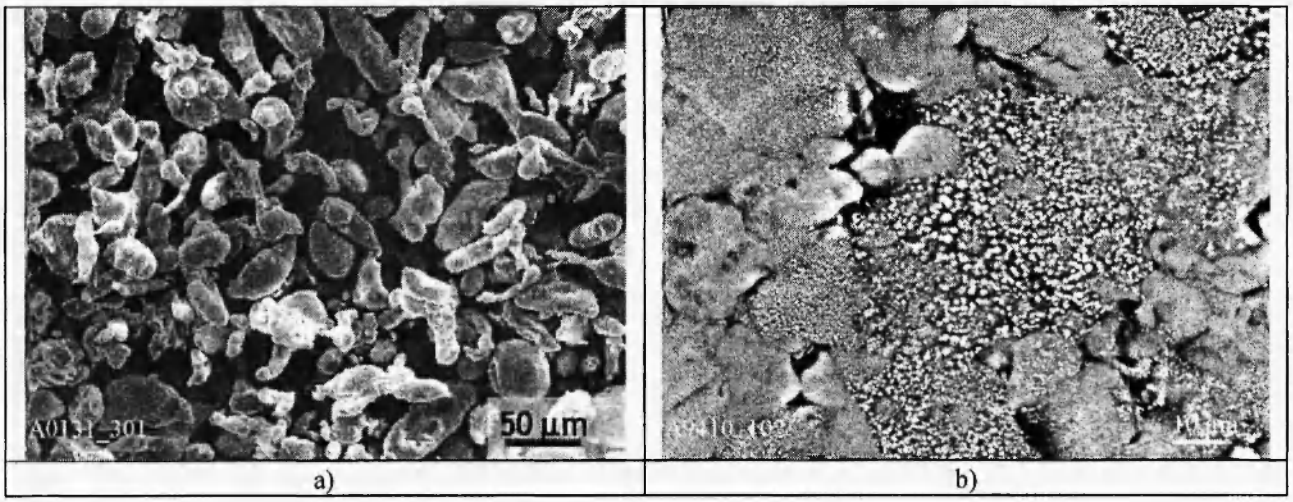

Fig. 1: SEM images of (a) morphology and (b) microstructure of as-atomised powder.

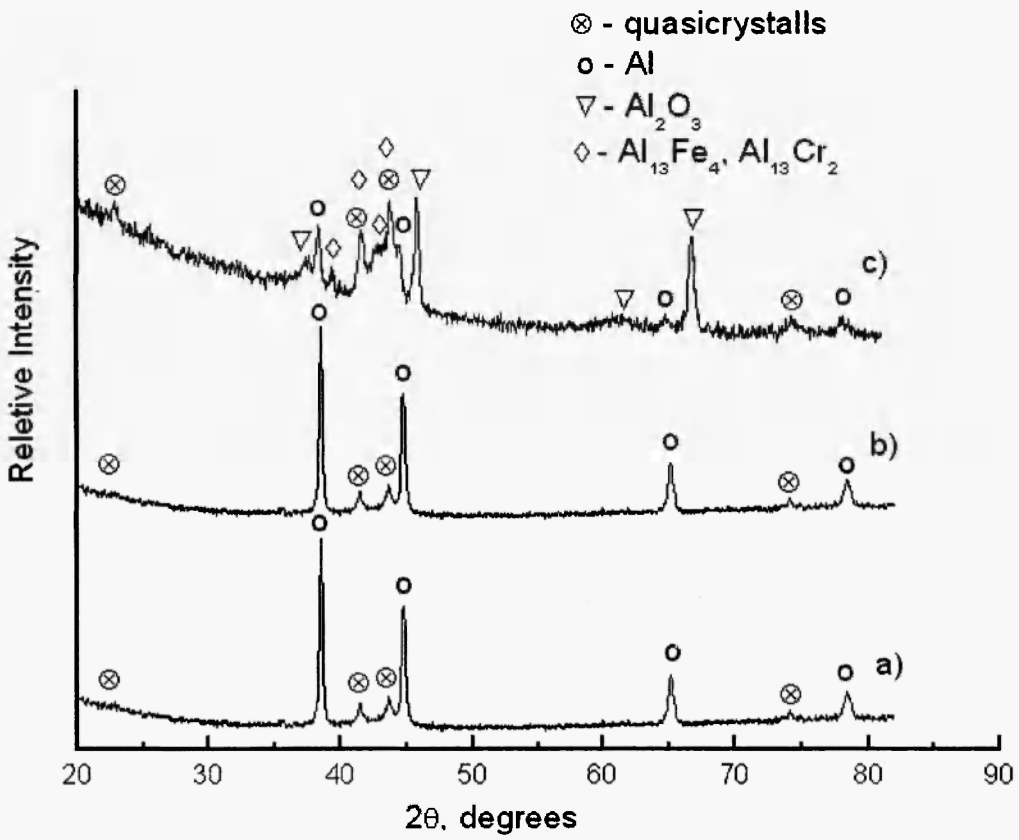

Fig. 2: XRD patterns of (a) the $Al_{94}Fe_{2.5}Cr_{2.5}Ti_1$-feedstock powder and (b, c) coatings performed by (b) cold spray technique and (c) HVOF spraying.

the interior of some powder particles, suggesting variable cooling conditions for water jets. By using XRD analysis volume fraction of quasicrystalline particles could generally be estimated roughly about 25 %, which is nearly the same as that published in /10/ for quasicrystalline alloys of the same nominal compositions.

As could be seen in **Figure 2b** no changes in intensity of diffraction peaks attributed to α-Al and i-phase presented in XRD patterns for cold-sprayed coatings are revealed, suggesting the maintenance of composite quasicrystalline structure the same as that of feedstock powder. Actually, huge numbers of white quasicrystalline particles within the feedstock powder particles are clearly visible in SEM images of the surface and cross-sectional microstructures of cold-sprayed coatings, shown in **Figure 3b**. Quasicrystalline nature of these particles is specified by the results of TEM observation. Typical TEM image of coating material and corresponding selected are of electron diffraction (SAED) is shown in **Figure 4**. Quasicrystalline particles with quite rounded shape are seen in TEM image while SAED pattern reveals five-fold spots indicative of i-phase.

The results testify that the thickness of cold-sprayed coatings varies from 750 to 800 μm and a few or no defects are visible at the interface with substrate, see **Figure 3a**. Apart from, no cracking and delaminating are observed in as-sprayed coatings. There are only some pores presented at the particle/particle interface at the porosity level that does not exceed 3%.

Generally, as-received cold-sprayed coatings demonstrate intimate bonding at the particle/particle and coating/substrate interfaces under strong impact despite of difficulties related to processing behaviour of Al-based feedstock powder. Compared to powder of pure metals and, in particular, Cu, Zn with high density and good deformability under sufficient kinetic energy [56], it is difficult to produce a dense Al-based coatings because of oxide film naturally presented on the surface of feedstock Al-powders and their low density /39, 24, 25/. In the present study, high strain rate lied in the region from 1.15×10^7 to $1.15 \times 10^5 s^{-1}$ and resulted from particle impact velocity estimated as high as 700 m/s /16, 38/ was quite enough to break off the surface oxide film and generate intimate metallurgical bonding between adjacent particles and substrate. Actually, remnant agglomerations of broken oxide layer are revealed by TEM observation at the particle/particle interfaces within coatings, as could be seen in **Figure 4a**.

Two different deformation processes ensure intimate bonding between particle surfaces cleaned from oxide layer. Severe plastic deformation of particles results in flattening and mechanical interlocking the splats by cold forging under high contact pressure estimated as great as 1.9 GPa /16/. **Figure 3** shows that in contrast to quasicrystalline particles, which keep unchanged morphology, feedstock powder particles exhibit irregular polyhedral shape only in coating surface whereas they are flattened and heavily deformed in cross-sectional microstructure. Powder particles get elongated lens-like shape with aspect ratio $k_f \approx 4.7$, indicating splat behaviour in solid state under impact.

The second deformation process is attributed to localised deformation at the particle/particle interfaces, resulting in so-called phenomenon as flow jet or adiabatic shear instability under high strain rate resulted from high impact velocity /57, 58, 59/. This bonding process is considered to be comparable to that in explosive welding or shock wave powder compaction /60, 61/. **Figure 3b** shows the evidences of intense shear localisation and those indicative of metallurgical bonding by impact fusion.

However, HVOF-sprayed coatings deposited using employed quasicrystalline feedstock powders is rather different compared to cold-sprayed coatings. Indications of partial transformation of metastable quasicrytalline i-phase into conversional intermetallic compounds with nominal compositions such as $Al_{13}Fe_4$ and $Al_{13}Cr_2$ are revealed in XRD pattern for HVOF-sprayed coatings, as could be observed in **Figure 2c**. This result is in good agreement with the data /62/ concerning partial transformation of i-phase into conventional intermetallic compounds resulted from plasma spraying the feedstock powder of quasicrystalline $Al_{83.7}Fe_7Cr_{6.3}Ti_3$ alloy attributed to Al-Fe-Cr-Ti system the same as that employed in the present study. Apart from, characteristic features of XRD pattern for HVOF-sprayed coatings are reduced intensity of diffraction peaks of α-Al and the presence of diffraction peaks attributed to aluminium oxide.

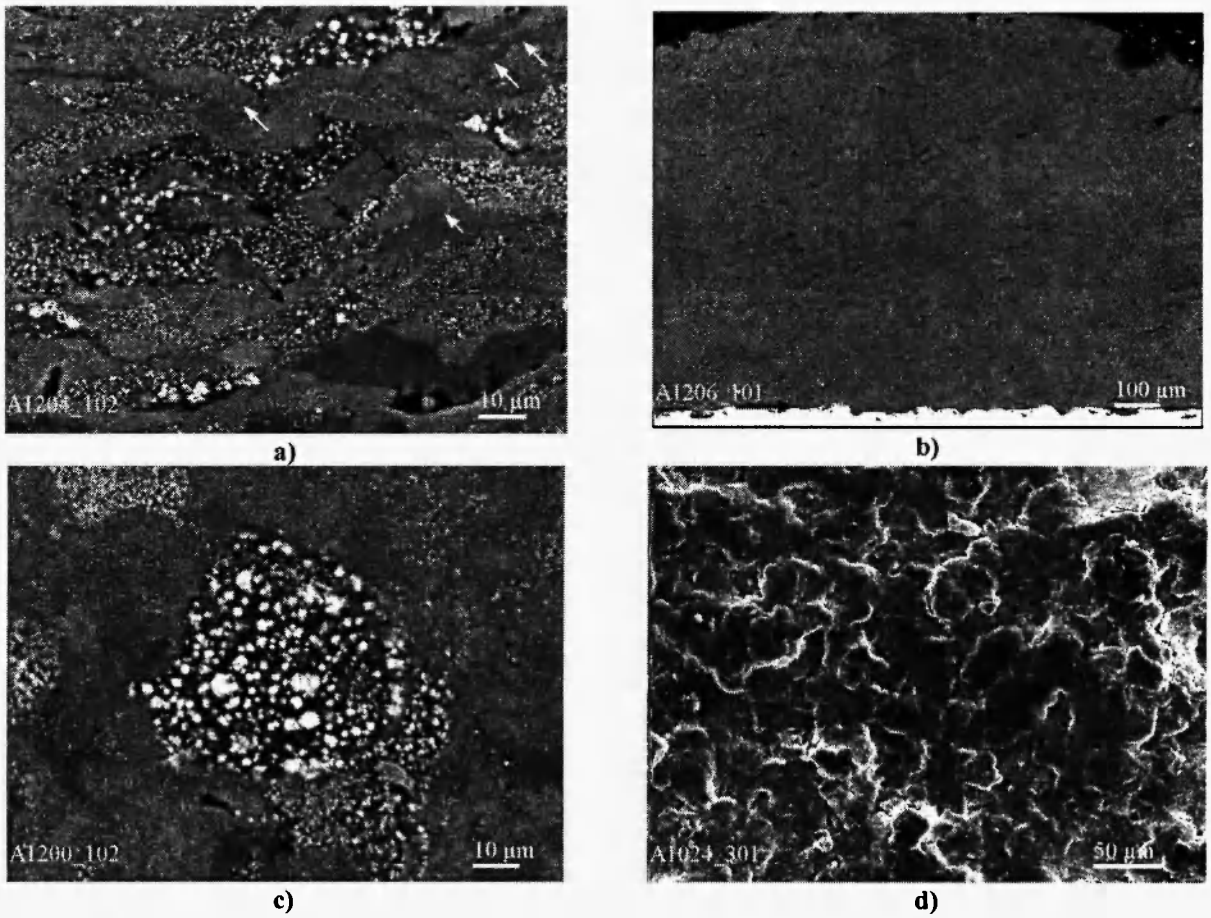

Fig. 3: SEM images of (a, b) cross-sectional and (c, d) surface microstructure of cold-sprayed coating performed by $Al_{94}Fe_{2.5}Cr_{2.5}Ti_1$-feedstock powder. The arrow in (b) indicates interface between coating and substrate material. Black arrows in (a) indicate the evidence of shear instabilities at the particle/particle boundaries whereas white arrows in (a) indicate the local metallurgical bonding between the powder particles.

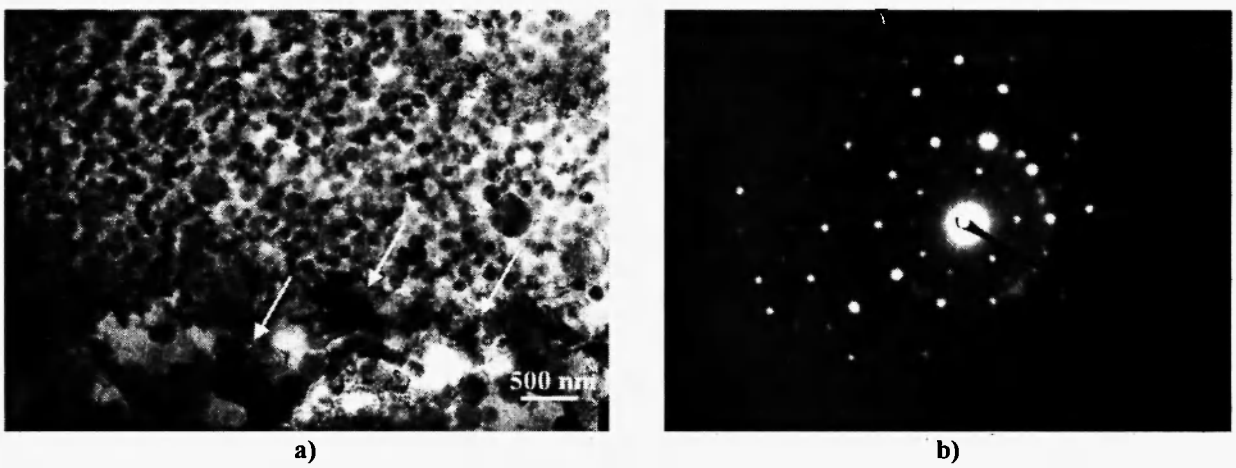

Fig. 4: (a) TEM image and (b) SAED pattern of cold-sprayed coating performed by $Al_{94}Fe_{2.5}Cr_{2.5}Ti_1$-feedstock powder. Arrows in (a) indicate the remnants of broken oxide layer.

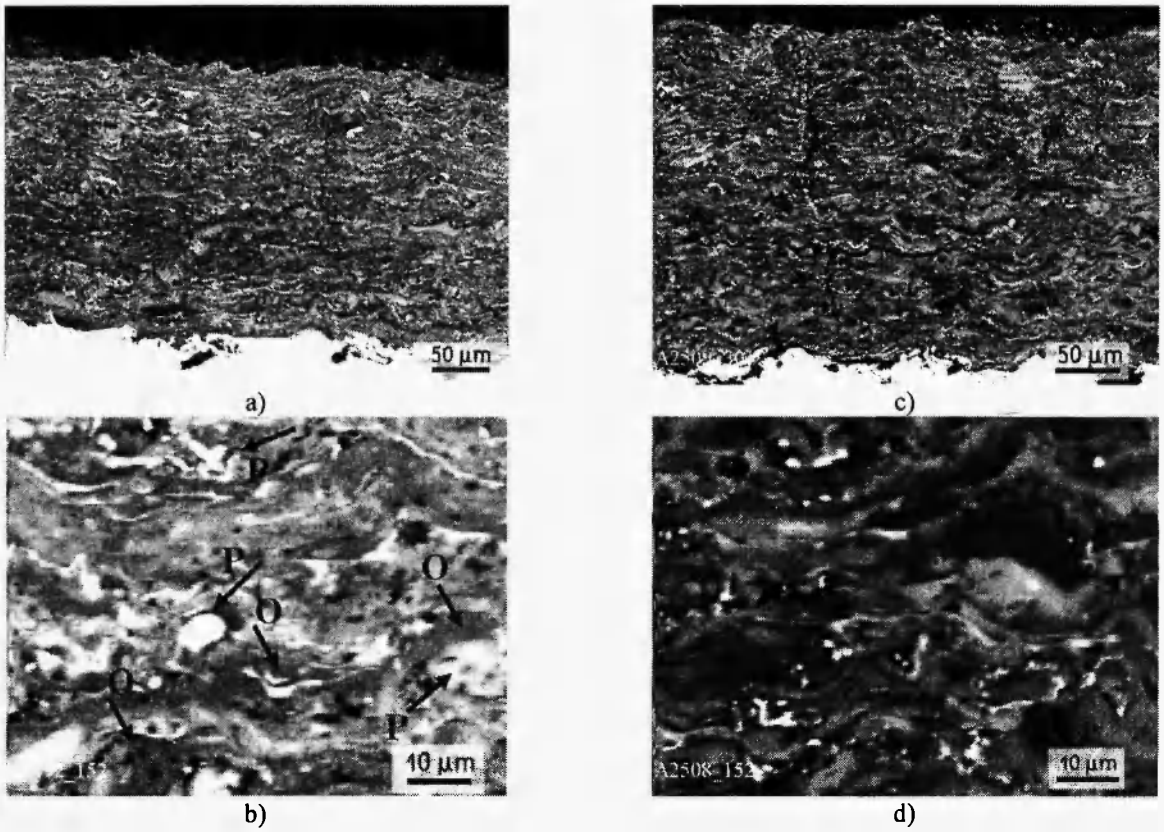

Fig. 5: SEM images of cross-sectional microstructure of HVOF-sprayed coating deposited using the feedstock powder of aluminium alloys with nominal compositions (a, b) $Al_{94}Fe_3Cr_3$ and (c, d) $Al_{94}Fe_{2.5}Cr_{2.5}Ti_1$. In (b) elongated splats of aluminium oxide (dark grey) are marked as O whereas particles of intermetallic compounds (white and light grey) are marked as P.

As could be seen in **Figure 5**, HVOF-sprayed coatings with the thickness about 500 µm show quite non-uniform microstructure consisted of lamellar like regions with rather different contours of contrast, indicating a steeper gradient in oxygen concentration dissolved within them. In addition, huge number of coarse and/or spheroidized particles compositionally corresponded to intermetallic compounds and splats of aluminium oxide are observed in the lamellar structure. It is noticed that the presence of small amount of titanium in composition of $Al_{94}Fe_{2.5}Cr_{2.5}Ti_1$-feedstock powder causes the oxidation level of HVOF-sprayed coating to rise up, resulting in reduced content of intermetallic compounds. Attention should be drawn to increased porosity level (between 5....7%) of HVOF-coatings, as shown in **Figure 5**. In addition, the presence of coarse brittle oxides and intermetallic compounds causes as-sprayed coatings to cracking and delaminating that crucially impair their structural performance, see **Figure 4a, b**.

Thus, the results of the present study show significant advantages of cold-sprayed technique compared to thermal spray processes and, in particular, to HVOF spraying. The main benefit of cold spraying is that the composite structure of initial feedstock powder of Al matrix alloy reinforced by metastable quasicrystalline particles is retained in coatings whereas microstructure of HVOF-sprayed coatings is highly supersaturated with oxygen and mainly dominated by oxides and conventional intermetallic compounds both formed in partially molten state during spraying as well as it is much impaired by increased porosity and local defects.

3.2 Mechanical Performance of Sprayed Coatings

Mechanical characteristics of feedstock powders as well as those of coatings performed by cold spray technique and HVOF spraying are listed in **Table 2**. It could be seen that the hardness HV of cold-sprayed coatings is higher roughly about by 2 times than that of corresponding feedstock powder, suggesting material strain hardening upon impact. Indeed, the presence of Ti in quasicrystalline alloy causes hardness numbers of feedstock powder and cold-sprayed coating, both performed by $Al_{94}Fe_{2.5}Cr_{2.5}Ti_1$-alloy, to be somewhat higher than those performed by $Al_{94}Fe_3Cr_3$-alloy. However, despite of increased hardness cold-sprayed coating performed by $Al_{94}Fe_{2.5}Cr_{2.5}Ti_1$-alloy shows the values of plasticity characteristics δ_H (δ_A) the same as those of cold-sprayed coating performed by $Al_{94}Fe_3Cr_3$-alloy. By considering the Eq. (1) it is easy to show that plasticity characteristic δ_H keeps the invariant value because the increased hardness number was balanced by increased value of Young's modulus, see **Table 2**.

Table 2
Mechanical characteristics of feedstock powders and coatings performed by cold spray (CS) technique and HVOF spraying

Mechanical parameter	Elementary composition of feedstock powder					
	$Al_{94}Fe_3Cr_3$			$Al_{94}Fe_{2.5}Cr_{2.5}Ti_1$		
	Powder	Coating		Powder	Coating	
		CS	HVOF		CS	HVOF
E, GPa	-	90.0±2.5	129±5.4	-	92.0±3.0	106±5.0
HV, GPa	0.91±0.3	1.95±0.12	5.00±0.4	1.03±0.3	1.99±0.14	5,10±0.35
δ_H	0.92	0.85	0.73	0.92	0.85	0.68
δ_A	-	0.87	0.78	-	0.86	0.73

Table 3
Cold spray gas conditions and adhesive strength of different cold-sprayed coatings

Powder	Propellant/ carrier gas	Gas pressure (MPa)	Gas temperature (° C)	Substrate	Adhesive strength (MPa)
Al-Cr-Fe alloy	Air/air	0.8	200	Cold-rolled steel	25±4
A2319 [39]	Air/ argon	2.8	560	Mild steel	34±4
Al12Si [39]	Air/ argon	2.7	520	Mild steel	> 50
Ti [39]	Air/ argon	2.8	520	Mild steel	15±4
Ti-6Al-4V [39]	Air/ argon	2.8	585	Mild steel	10±2
Cu [41]	Nitrogen/ nitrogen	3.0	305	Low carbon steel	10
Cu* [41]	Nitrogen/ nitrogen	3.0	305	Low carbon steel	27

Notice: * annealed state (1 h/400° C)

It is noticeable that plasticity characteristics δ_H (δ_A) for both kinds of feedstock powders are greater than critical value $\delta_H \geq 0.9$, indicating ductile behaviour of material in conventional tensile and bending tests /49/ and, therefore, ensuring its good deformability under impact. That is why no evidences of delaminating and cracking have been observed in microstructure of as-received cold-sprayed coatings, see **Figure 3**. It is also essential that both kinds of cold-sprayed coatings keep the values of plasticity characteristics δ_H (δ_A) just about critical value, implying their workability under loading during exploitation /48/.

HVOF-sprayed coatings demonstrate the values of Young's modulus and hardness, which much superior to those of cold-sprayed coatings their plasticity characteristics δ_H (δ_A) are too small and indicative of tendency to brittle fracture /48, 49/. Actually, cracking and delaminating have been typically observed in the microstructure of as-received HVOF-coatings, see **Figure 5**. In addition, as opposed to cold-sprayed coating the presence of Ti in composition of feedstock powder leads to decreasing the plasticity characteristics δ_H (δ_A) of HVOF-coating. Following to above explanation using the Eq. (1) it is understanding that decrease of Young's modulus is primary responsible for decreasing the plasticity characteristics δ_H when no change of hardness number occurs, see **Table 2**.

Thus, with a view to damage tolerance the essential benefit of cold sprayed coatings based on Al matrix and reinforced by quasicrystalline particles is providing the combination of relatively high hardness and high ductility. It is important, that quasicrystalline Al alloys in systems Al-Fe-Cr/Al-Fe-Cr-Ti exhibit the thermal stability of mechanical properties at least up to 300° C /10/, making the cold-sprayed coatings valuable for application in aircraft industry.

Besides mechanical properties bond strength plays crucial role in mechanical performance of sprayed coatings. The results listed in **Table 3** show that quasicrystalline coating cold-sprayed on cold rolled steel substrate demonstrate quite high value of adhesive strength although it is lower than that reported in literature for other Al-based coatings cold-sprayed on the middle steel plates. However, bond strength of Al-based quasicrystalline coatings is much higher than that for Ti – based coatings cold-sprayed on the middle steel substrate.

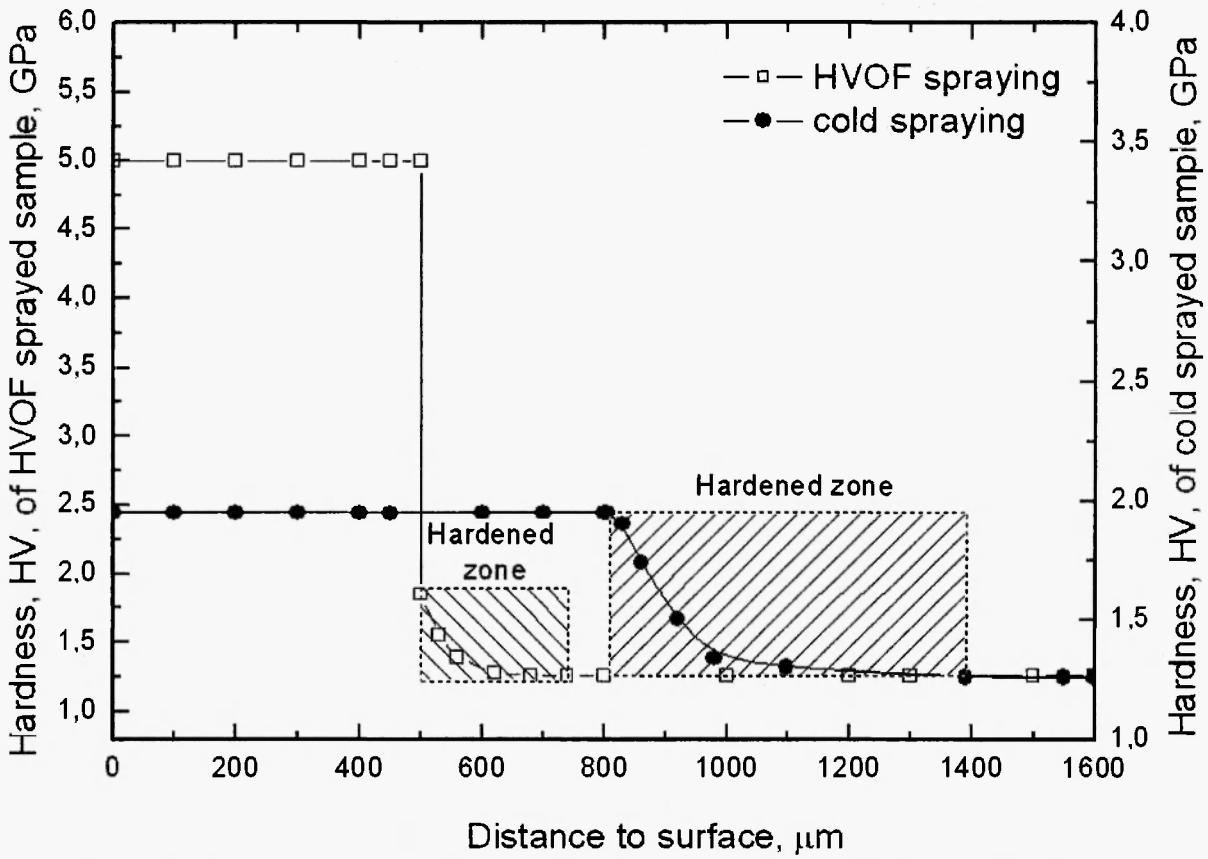

Fig. 6: Vickers hardness, HV, across cross-sectional structures of cold-rolled steel processed with feedstock powder of $Al_{94}Fe_3Cr_3$ alloy by using cold spray technique and HVOF spraying.

The differences in adhesive strengths could be ascribed to the differences in strength properties of substrate material and processing parameters used in cold spraying. In particular, bond strength is usually higher on soft substrate materials. For instance, adhesion of copper coating cold-sprayed on steel substrate with nitrogen as process gas does not exceed 10 MPa in the as-sprayed state whereas its bond strengths on aluminium and copper substrates achieve 44 and 38 MPa respectively, as was reported in /63/. Therefore, lower bond strength of cold-sprayed quasicrystalline coatings could be resulted from high hardness of cold-rolled steel substrate. In addition, steel substrate experiences significant strain hardening under impact, as could be seen in **Figure 6**. Hardness of substrate zone adjacent to coating increases by 50% and reaches the value nearly the same as that of quasicrystalline coating. Then hardness decreases gradually toward the centre of substrate. After cold spraying the thickness of hardened zone in substrate reaches about 600 μm. Improvement of cold-sprayed coatings could be provided by annealing a steel substrate before spraying.

HVOF-spraying leads also to strain hardening the steel substrate, as shown in **Figure 6**. The difference is that the extension of hardened zone resulted from HVOF-spraying is smaller by 4 times although the hardness of substrate zone adjacent to coating is roughly the same as that after cold spraying. However, strain hardening the substrate is of resulted from high velocity of gas-particles flow. Cold-sprayed coatings exhibited flattened and heavily deformed powder particles with aspect ratio $k_f \approx 4.7$ whereas quasicrystalline particles in their interior kept unchanged morphology.

Effective metallic bonding between the adjacent particles by breaking off the oxide films presented on the feedstock Al-powder and intimate contact between clean surfaces by mechanical interlocking and even by impact fusion was found to be indicative of the cold-sprayed coatings. Apart from, no cracking and delaminating are demonstrated in cross-sectional microstructure and at the coating-substrate interface whereas the defects above were revealed in HVOF-sprayed coatings due to the presence of brittle oxides and intermetallic compounds.

Overall, strain hardening resulted in increased hardness of cold-sprayed coatings which superiors small significance because of HVOF-spraying can guarantee high bond strength due to at least partially molten state of sprayed particles. Unfortunately, despite of high hardness and high adhesive strength, cracking and delaminating resulted from low ductility impairs the mechanical performance of as-received HVOF-coatings, making them unserviceable for further engineering application.

4. CONCLUSIONS

By using feedstock powders with nominal compositions such as of $Al_{94}Fe_3Cr_3$ and $Al_{94}Fe_{2.5}Cr_{2.5}Ti_1$ the present study demonstrate significant advantages of cold-spraying in performance of Al-based coatings reinforced by metastable nano- and submicrometer-sized quasicrystalline particles as compared to thermal spray processes and, in particular, to HVOF spraying.

The main benefit of cold spraying is that the composite quasicrystalline structure of initial feedstock powder is retained in coatings whereas microstructure of HVOF-sprayed coatings was dominated by conventional intermetallic compounds and aluminium oxides embedded in Al matrix highly supersaturated with oxygen. At the porosity level limited to 3% microstructure of cold-sprayed coatings was mainly affected by intensive plastic deformation under impact nearly by 2 times to that of corresponding feedstock powder. The important point is that the plasticity characteristics δ_H (δ_A) of feedstock powder and coatings were determined to be just about critical value $\delta_H \cong 0.9$ indicated in literature /49/ as criterion for ductile behaviour of material under conventional tensile and bending tests and, thus, quite enough for preventing cold-sprayed coatings against brittle failure during particle impact onto substrate or previously deposited particles.

Adhesive strength of cold-sprayed coatings was determined to be about 25 MPa that is relatively high taking into account the high hardness of cold-rolled steel substrate. Due to strain hardening under impact hardness of substrate zone adjacent to coating increased by 50% and reached the value nearly the same as that of quasicrystalline coating. Despite of HVOF-sprayed

coatings could guarantee higher bond strength due to at least partially molten state of sprayed particles and give the hardness increased by roughly about two and half times compared to cold-sprayed coatings they showed rather low values of plasticity characteristics $\delta_H \cong \delta_A \cong 0.7$, indicating their tendency to brittle fracture and making them unserviceable for further engineering application.

ACKNOWLEDGEMENT

Significant parts of the research were supported by the Programme of Ukrainian Academy of Sciences for nanosystems, nanomaterials, and nanotechnologies. Spe cial thanks to Dr. O.D. Neikov for performance of the quasicrystalline feedstock powders, Dr. M.O. Iefimov for the help with XRD analysis, Dr. N. I. Danylenko and Mr. A. V. Sameliuk for the help with electron microscopy, and Dr. V. F. Gorban for load-displacement measurements.

REFERENCES

1. Shechtman D., Blech., Gratias D. and Cahn J.V., *Phys Rev Lett.* **53**(20), 1951-1954 (1984).
2. J.-M. Dubois, *Introduction to quasicrystals*, Berlin: Springer Verlag, 392p. (1998).
3. Adeeva L.I., Borisova A.L., *Physics and chemistry of solid body.* **3**(3), 454-465 (2002.).
4. E. Hornbogen and M. Shandl, *Z. Metallkd,* **83**, 128-131, (1992).
5 J.M. Dubois, S.S. Kang and Y. Massiani, *J. of Non crystalline Solids*, **153-154**, 443-445 (1993).
6. S. S. Kang, J. M. Dubois, and J. von Stebut, *J. Mater. Res.* **8**(10), 2471-2481, (1993).
7. A. Rudiger, and U. Koester, *Mater. Sci. Eng.* **294**(296), 890-903 (2000).
8. Kimura H.M., Sasamori K. and Inoue A., *J. Mater. Res.* **5**(12), 2737-2744 (2000).
9. Sasamori K. and Inoue A., *J. Mater. Res.* **15**(12), 2737-2744 (2000).
10. Yu. V. Milman, A.I.Sirko, M.O.Iefimov, O.D.Neikov, A.O.Sharovsky, and N.P.Zacharova, *High temperature materials and processes.* **25,** 19-29 (2006).
11. Inoue, A. *Progress in Mater. Sci.* **43**, 365-520 (1998).
12. Inoue A. and Kimura H.M., *J. Mater. Res.* **11**(2), 221-231 (1999).
13. Inoue A. and Kimura H.M., *J. Mater. Res.* **15**(12), 2737-2744 (2000).
14. M.O.Iefimov, D.V.Lotsko, Yu.V.Milman, A.L.Borisova, S.J. Chugunova, Ye.A. Astakhov and O.D.Neikov, *High temperature materials and processes,* **25**, 31-39 (2006).
15. A. Inoue and H. Kimura, *Mater. Sci. Eng.* **A286**(1), 1-10 (2000).
16. M.V. Semenov, M.M. Kiz, M.O. Iefimov, A.I. Sirko, A.V. Byakova, and Yu.V. Milman, *Nanosyst., Nanomat., Nanotekh.* **4,** 767-783 (2006).
17. Yu. V. Milman, *Materials Science Forum*, **482**, 77-82 (2005).
18. A. Ziani, A. Pianelli, A. Redjiamia et al., *J. Mater Sci,* **30**, 2921-2929 (1995).
19. C. Zhang, Y. Wu, Y. Cai. Et al, *Mater. Sci. Eng.* **A323**, 226-231 (2002).
20. K.N. Ishihara, S.R. Nishitani and P.H. Shingu, *Transactions ISIJ.* **28**, 1-6 (1988).
21. H. Lones, *Rep. Prog. Phys.* **36**(11), 2435-2497 (1973).
22. J.Gurland and N.M. Parih, in: *Fracture Advanced Treatise.* Part 2 *(Ed. H. Liebowitz)* N.Y.-London: Academic Press, 472 (1972).
23. Karpetz M.V., Firstov S.A., Kulak L. D., et al. *Physics and chemistry of solid body.* 7(1), 147-151 (2006).
24. K. Urban, M. Moser, *Phys. Stat. Sol. (a)*, **91**, 411-422 (1985).
25. C. Banjongprasert, S.C. Hogg, I.G. Palmer et al., *Mater. Sci., Forum*, **561-565**, 1075-1078 (2007).
26. Pat. 5432011 US. Aluminum alloys, substrates coated with these alloys and their applications / J.M. Dubois, A. Pianeli. – Publ. 11.07.95.
27. Sordelet D.J., Kramer M.J. and Unal O., J. *Thermal Spray Techn.* **4**(3), 235-244 (1995).
28. Dobois J.-M., Proner A., Bucaille B. et al. *Ann. Chim. Fr.* **19**, 3-25 (1994).
29. D.J. Sordelet, P.D. Krotz, R.L. Daniel Jr. and M.F. Smith., *Proceedings of the 8-th International Thermal Spray Conference,* 11-15 Sept. 1995, Houtson, Texas, p. 627-632 (1995)
30. D.S. Sordelet, M.F., Besser and I.E. Anderson *J. of Thermal Spray Technology*, **5**(2), 161-173 (1996).

31. D. Sordelet and M. Besser., *Proc. of NTSC 96. (ed. C.C.Bernd),* Publ. by Asm International, Materials Park, Ohio-USA, *1996,* p. 419-428 (1996).
32. M.O.Iefimov, D.V.Lotsko, Yu.V.Milman, A.L.Borisova, S.J. Chugunova, Ye.A. Astakhov and O.D.Neikov, *High temperature materials and processes.* **25**, 31-39 (2006).
33. J.M. Dubois, S.S. Kang and Y. Massiani, *J. of Non crystalline Solids*, **153-154**, 443-445 (1993).
34. J.R. Davis, *Handbook of Thermal Spray Technology*, 338 p, (2004).
35. A. Papyrin, V. Kosarev, S. Klinkov, A. Alkhimov and V. Fomin *Cold Spray Technology, Elsevier Science*, 336p. (2006).
36. T. Stoltenhoff, H. Kreye and H.J. Richter, *J. Therm. Spray. Technol.*, **11**, 542-550 (2002).
37. F. Gartner, T. Stoltenhoff,, I. Voyer, H. Kreye,, S H. Kreye,. S. Riekehr and M. Kosak, *Surf. Coat. Technol.* **200**, 6770-6782 (2006).
38. B. Jodoin, L. Ajdelsztain, E. Sansoucy, A. Zuniga, P. Richer and E.J. Lavernia, *Surf. Coat. Technol.* **201**, 3422-3429 (2006).
39. Wen-Ya Li, Chao Zhang, Xueping Guo and Chang-Jiu Li, *Appl. Surf. Sci.* **254**(2), 517-526 (2007)
40. Xian-Jin Ning, Jae-Hoon Jang, Hyung-Jun Kim, Chang-Jiu Li and Changhee Lee, *Surf. Coat. Techno.* **202**(9), 1681-1687 (2008).
41. T. Stoltenhoff, B. Borchers, F. Gartner and H. Kreye, *Surf. Coat. Technol.* **200**, 4947-4960 (2006).
42. C.-J. Li, W.-Y. Li and H.L. Liao, *J. Therm. Spray. Technol.* **15**, 212-222 (2006).
43. W.-Y. Li, C. Zhang, X.P. Guo, H.L. Liao and C. Coddet, *Appl. Surf. Sci.* **253**(17), 7124 -7130 (2007)
44. L. Ajdelsztain, B. Jodoin, G.F. Kim and J. M. Schoenung, *Met. Mat. Trans, F* **36**(3), 657-669, (2005)
45. Neikov O.D., Kalinkin V.G., et al. Patent Ru # 2078427, Information Bulletin No. 12, 1977.
46. L. Ajdelsztain, A. Zuniga, B. Jodoin and E.J. Lavernia, *Surf. Coat. Technol.*, 201, 1166-1178, (2006)
47. Byakova A. V., Milman Yu. V. and Vlasov A.A., *Nanophysics, nanosystems, and nanomaterials.* **2**(1), 215-225 (2004).
48. Byakova A. V., Milman Yu. V. and Vlasov A.A., *Science of Sintering.* **36**, 27-41 (2004).
49. Yu. V. Milman, B. A. Galanov and S.I. Chugunova, *Acta. Metall. Mater.* **41**(9), 2523 (1993).
50. Oliver W.C. and Pharr G.M., *J. Mater. Res.* **7**(6) 1564-1583 (1992).
51. Byakova A.V., Milman Yu.V. and Vlasov A. V. in: *Modelling of Machining Operations* (ed. R. Neugebauer), Chemnitz: Wissenschaftliche Scripten, p. 559-568 (2005).
52. Yu.V. Milman. J. Phys. D: *Appl Phys.* **41**, 1-9 (2008).
53. Milman Yu. and Dub S., Golubenko A.. *Mater. Res. Soc. Symp.*, Proc. **1049**, 123-128 (2008).
54. Yu.V. Naidich, V.P. Umanskii and I.A. Lavrinenko, *Strength of the diamond-metal interface and brazing of diamonds*, Cambridge: International Science Publishing, 160 p. (2007).
55. M. Yamasaki, Y. Nagaishi and Y. Kawamura, *Scripta Mater.* **56**, 785-788 (2007).
56. T.Schmidt, F.Gartner, H.Assadi and H.Kreye, *Acta Mater.* **54**, 729 (2006).
57. M. Grujicic, J.R. Saylor, D.F. Beasley, W.S. DeRosset and D. Helfritch, *Appl. Surf. Sci.* **219**(3-4), 211-227 (2003).
58. R.C. McCunc. W.T. Donlon, O.O.Popola and E.L. Cartwright, *J. Therm. Spray Technol.* **9**, 73-89 (2000).
59. W.-Y. Li, H.L.Liao, C.-J. Li, C.Coddet and X.F. Wang, *Appl, Surf. Sci.* 253, 2852 (2006).
60. H. El-Sobky, in *Explosive Welding, Forming and Compaction* (ed. T.Z. Blazynski), London-N. Y.: Applied Science Publishers, p. 189-216 (1983).
61. Gas thermal spraying of composite coatings/ A.Ya. Kulik, Yu.S. Borisov, A.S, Mnuhin, M.D. Nikitin, Leningrad: Mashinistroenie, 199 p. (1985) (Rus.).
62. Yeong-wook Kim, Hee-Jung Kim and Hyun-Myung Shin, *Solid State Phenomena*, 124-126, 1601-1604 (2007).
63. L. Ajdelsztajn, A. Zuniga, B. Jodoin and E.J. Lavernia, *Surf. Coat. Technol.* **201**(12), 2109-2116 (2006).